RSC Advances

PAPER

View Article Online
View Journal | View Issue

Cite this: RSC Adv., 2017, 7, 16131

Effects of organic solvents on the structures of micellar nanocrystals†

Xinyi Ding,[ab] Ning Han,[ab] Jun Wang,[ab] Yuxiang Sun[ab] and Gang Ruan*[ab]

Micellar nanocrystals (nanocrystal-encapsulated micelles) has become an emerging class of nanomaterials for a wide spectrum of biomedical applications. The most commonly used approach to vary the properties of micellar nanocrystals is using different types or molecular weights of amphiphilic molecules. The present work focuses on investigating the effects of an alternative material parameter, *i.e.*, organic solvent, which primarily affects the kinetics rather than thermodynamics of the formation process, on the structures of the micellar nanocrystal product fabricated by combining electrospray and self-assembly. We find that, compared with chloroform (commonly used in prior works and used as the reference here) as the organic solvent, dichloromethane (DCM, lower boiling point than chloroform) leads to nearly zero encapsulation of nanocrystals in micelles, and tetrahydrofuran (THF, higher water miscibility than chloroform) leads to greatly enhanced encapsulation of nanocrystals in micelles. The use of THF could thus solve the previously identified problem of low nanocrystal encapsulation. Surprisingly, a prolonged fabrication process of micellar nanocrystals with THF is found to generate worm-shaped products. Further study of the formation mechanism of the worm-shaped micelles indicates that they are formed through THF-induced/facilitated fusion of spherical micelles. The thus-formed worm-shaped micellar nanocrystals are found to offer greatly reduced non-specific cellular uptake than the spherical counterparts. These results offer significant insights on micellar nanocrystal, micelle fusion as well as self-assembly, and provide new ways to control the structures of nanomaterials and their biological responses.

Received 27th December 2016
Accepted 8th March 2017

DOI: 10.1039/c6ra28741g

rsc.li/rsc-advances

Introduction

In the past twenty years a large variety of nanometer-sized materials, such as semiconductor quantum dots, iron oxide nanoparticles and gold nanoparticles, have been introduced to interface with biological systems for biomedical applications.[1–6] A commonly used strategy of solubilizing nanomaterials in aqueous environments, which is generally required for interfacing with biological systems, is to use micelles to encapsulate hydrophobic nanocrystals.[3,6] A micelle is a classic self-assembly system spontaneously formed after certain amphiphilic molecules (small molecules or polymers) are dispersed in an aqueous environment. Micelles have been widely used as cleaning agents and delivery vehicles of small molecule drugs due to the ability of micelles to encapsulate hydrophobic molecules in the micelle core.[7] In 2002, Dubertret *et al.* reported the first micelle encapsulation of hydrophobic nanocrystals, with each micelle generally encapsulating a single nanocrystal, and the application of nanocrystal-encapsulated micelles in biological imaging.[8] More recently, a number of research groups have successfully used micelles to encapsulate multiple hydrophobic nanocrystals per micelle.[9–11] The need for a micelle encapsulating multiple nanocrystals primarily comes from applications in integrating dual-functions or multi-functions (*e.g.* both fluorescence and magnetism) of constituent nanocrystals (*e.g.* semiconductor quantum dots and superparamagnetic iron oxide nanoparticles) into a single nano-platform (*i.e.* composite nanoparticle),[9,11–16] or/and in combining different colors of the same type of constituent optical nanocrystals,[10] or/and in enhancing signal by concentrating multiple constituent nanocrystals into a single micelle.[10]

From a fundamental point of view, a nanocrystal-encapsulated micelle (also called micellar nanocrystal in the present work) is significantly different from a micelle alone (also called an 'empty micelle' here) or a micelle encapsulating small molecules (*e.g.* drugs). The differences could arise from thermodynamics or/and kinetics. In the thermodynamics, both the enthalpy and entropy changes of the process of encapsulating nanocrystals into a micelle could differ significantly from those of encapsulating small molecules; in the kinetics, the transport of nanocrystals could differ significantly from that of small molecules.[17–21] The commonly used method to vary the properties of micellar

[a]Department of Biomedical Engineering, College of Engineering and Applied Sciences, Nanjing University, China. E-mail: gangruan@nju.edu.cn
[b]Collaborative Innovation Center of Chemistry for Life Sciences, Nanjing University, China

† Electronic supplementary information (ESI) available. See DOI: 10.1039/c6ra28741g

nanocrystal is by changing the amphiphilic block polymer (type or molecular weight of the polymer) used to form micelles.[9–12] In the present work, we investigate the effects of an alternative parameter, *i.e.*, organic solvent, on the formation of micellar nanocrystals, with focus on the structural properties, such as encapsulation number and micelle morphology, of the product. Although the effects of organic solvents on the formation of empty micelles have been previously investigated,[22] these effects have rarely been studied for micellar nanocrystals. Because the organic solvent is expected only to affect kinetics (rather than thermodynamics) of the assembly process as it is eventually removed from the assembly system by evaporation, investigating the effects of organic solvent would especially offer insights into the kinetics, including its relative importance compared with the thermodynamics, of the assembly process of micellar nanocrystals.

Experimental section

Materials

Hydrophobic quantum dots (QDs) (fluorescent emission peak wavelength = 605 nm) were purchased from Ocean Nanotech. Poly(styrene-*b*-ethylene glycol) (PS–PEG) and PS–PEG–COOH (the molecular weight of PS segment is 9.5 kDa and that of PEG segment is 18.0 kDa, respectively) were purchased from Polymer Source. Poly(vinyl alcohol) (PVA) (molecular weight 13–23 kDa, 87–89% hydrolyzed) was purchased from Sigma-Aldrich. The organic solvents were purchased from Sinopharma Chemical Reagent. The hydrophobic fluorescent dyes (the dialkylcarbocyanine family) for colocalization studies were purchased from KeyGENBioTECH. Tat peptide was purchased from ChinaPeptides. 2-(*N*-Morpholino)ethanesulfonic acid (MES) buffer, *N*-hydroxysulfosuccinimide (NHS) sodium salt, *N*-(3-dimethylaminopropyl)-*N*′-ethylcarbodiimide (EDC) were purchased from Aladdin. HeLa cells and their culture medium were purchased from KeyGENBioTECH.

Fabrication of micellar nanocrystals

Nanocrystal-encapsulated micelles (micellar nanocrystals) were prepared by a method combining electrospray and self-assembly. The details of the principle and operation of this process are described previously.[23] In this process, electrospray is used to form uniform and small oil-in-water emulsion droplets (the oil phase contains amphiphilic block copolymer PS–PEG, hydrophobic nanocrystals QDs and organic solvent; the water phase contains the surfactant PVA and water); subsequently the organic solvent in the emulsion droplets is evaporated, which induces self-assembly mainly due to hydrophobic interaction and forms nanocrystal-encapsulated micelles. Here, the electrospray setup has a coaxial configuration. The inner capillary needle was a 27 gauge (outer diameter 500 μm; inner diameter 300 μm) stainless steel capillary, and the outer needle was a 20 gauge (outer diameter 1000 μm; inner diameter 500 μm) stainless steel three-way connector. The nozzle tip was positioned 0.8 cm above a grounded steel ring and 10 cm above a glass collection dish. The oil phase was delivered to the inner stainless steel capillary at a flow rate of 0.6 ml h^{-1} using a syringe pump (SPLab01, Shenzhen, China). The concentrations of PS–PEG and QDs in the oil phase were 5 mg ml^{-1} and 0.25 mg ml^{-1}, respectively. An aqueous phase was prepared by dissolving PVA in deionized water at 40 mg ml^{-1}. The aqueous solution was delivered to the outer annulus of the coaxial needle at a flow rate of 1.5 ml h^{-1} using a second syringe pump (SPLab01, Shenzhen, China). The glass collection dish contained 10 ml of deionized water. Taylor cone of electrospray typically appeared at a voltage of 6–7 kV. For the experiments involving timing the "reaction" of micellar nanocrystal formation, timing was started when the Taylor cone was observed to have formed at the tip of the electrospray apparatus. Finally, the dispersion in the glass collection dish was transferred to a 15 ml centrifuge tube for characterizations, applications, or storage.

Transmission electron microscopy (TEM)

Images of micelles were obtained using a JEM-2010 TEM. First, after the micelle sample was sonicated for 2 min, 10 μl droplets of sample were pipetted onto the formvar/carbon-coated nickel grid, waiting for 2 min to let the water evaporate. Subsequently 10 μl droplets of phosphotungstic acid (PTA, 1%) solution were pipetted onto the formvar/carbon-coated nickel grid. Negative staining with PTA was performed for 2 min, and the excess liquid was wicked away. The grid was then imaged. For analysis of particle size or encapsulation number of a particular formulation of micelles (including nanocrystal-encapsulated micelles), two or three micelle samples were prepared separately under identical experimental conditions. For each micelle sample, 10–20 images were captured from randomly selected views, and totally 100–300 micelles were measured for encapsulation number (measured by counting number of nanocrystal in a micelle) and particle size (measured by using the Image J software). To obtain the mean values and standard deviations of encapsulation number and particle size of the particular formulation of micelles, the results from the two or three separate micelle samples (prepared under identical experimental conditions) were combined.

Dynamic light scattering (DLS)

Hydrodynamic particle size was characterized using dynamic light scattering (HITACHI F-4600). Samples were taken from the micelle suspensions described above and diluted with distilled water if necessary to reduce the intensity of scattered light to the acceptable range of the instrument. Mean particle diameters weighted by number were recorded.

Fluorescent spectrophotometer

The fluorescence spectra were obtained using a fluorescence spectrophotometer (HITACHI F-4600). The PMT voltage used was 700 V and the scan speed used was 1200 nm min^{-1}.

Thermogravimetric analysis

The chemical compositions of samples of micellar nanocrystals were analyzed by a Thermal Gravimetric Analyzer (Pyris 1 DSC

PerKin Elmer). The protective gas used was nitrogen and the rate of temperature change was 20 °C min^{-1}.

Colocalization study for the formation mechanism of worm-shaped micelles

A green hydrophobic fluorescent dye and an orange hydrophobic fluorescent dye (the dialkylcarbocyanine family, with the colors being from the fluorescent emissions) were used in the micelle fabrication process to label the cores of micelles in a sequential manner, and by studying the colocalization of the two different fluorescent colors, to examine whether fusion of different micelles labeled with different fluorescent colors had occurred. In the initial 30 min of electrospray, the green hydrophobic fluorescent dye (in addition to PS–PEG) was used in the oil phase flow. Then, after the initial 30 min the dye used was switched to the orange fluorescent dye. The molar concentrations of the dyes used in the experiments of fabricating dye-encapsulated micelles were the same as those of QDs used in the fabrication of QD-encapsulated micelles.

The formed micelles, which were diluted 200 times by deionized water, were then observed by confocal fluorescence microscopy (Olympus IX-83 epi-fluorescent microscope, Andor spinning disk confocal system, Photometrics DV2 dual channel simultaneous imaging system, and Photometrics Evolve 512 EMCCD camera). The excitation wavelength used was 488 nm. The dual channel emission filters used in the DV2 system had the following two different wavelength ranges: 500–500 nm (green) and 581–653 nm (orange-red). Control experiments were performed to ensure that the fluorescence of the green hydrophobic fluorescent dye only appeared in the green channel of the DV2 imaging system (no significant signal detected in the orange-red channel), and the fluorescence of the orange hydrophobic fluorescent dye only appeared in the orange-red channel of the DV2 imaging system (no significant signal detected in the orange-red channel).

Imaging of cellular uptake of Tat peptide-conjugated micellar nanocrystals

Conjugation of Tat peptide with micellar QDs (part of PS–PEG was replaced by PS–PEG–COOH) was conducted by the well-established EDC/NHS coupling reaction. In a typical procedure of the conjugation, the micellar QDs and EDC/NHS were mixed in 10 mM MES buffer (pH = 6) for 15 min, and Tat peptide was added and the conjugation reaction was allowed to continue for 10 h.

HeLa cells (KeyGENBioTECH) were seeded on glass-bottom tissue culture plates at an initial confluency of 20% in 600 μl of medium (DMEM + 10% fetal bovine serum) and were cultured for 40 h in 5% CO_2 at 37 °C. Micellar QDs at a given concentration were then added. After being incubated with micellar QDs for a specific time duration, the cells were washed twice with fresh culture medium to remove free micellar QDs, and the cells were imaged by a live cell confocal microscopy system, which consists of a cell incubation chamber (IX3W, Tokai Hit), an epi-fluorescent microscope (IX-83, Olympus, with halogen lamp as the light source), a spinning disk confocal system (Andor) and an electron multiplying charge-coupled device (EMCCD) camera (Evolve 512, Photometrics).

Results and discussion

Quantum dots (QDs), *i.e.* semiconductor nanocrystals that can emit strong and stable size and composition-dependent fluorescence,[1,2] were used in the present work as the model hydrophobic nanocrystals. Micellar nanocrystals in the present work were prepared by a semi-continuous production process combining self-assembly with electrospray, as described previously.[23] A primary feature of this process is that electrospray is used to generate uniform oil-in-water emulsion droplets which, upon the removal of organic solvent by evaporation, undergo self-assembly driven mainly by hydrophobic interaction and form micellar nanocrystals.[24,25] In the previous work the organic solvent used was typically chloroform, and it was found that a major unresolved problem was low encapsulation, *i.e.*, only a small percentage of micelles contained nanocrystals.[23] Here we use chloroform as the reference point, and examine primarily the use of two different solvents in comparison with chloroform. These two different solvents are selected with the goal of studying the effects of two specific solvent properties, namely boiling point and miscibility with water, respectively. The two different solvents examined in the present work are as follows: (1) dichloromethane (DCM), which has substantially lower boiling point than chloroform (40 °C for DCM and 61 °C for chloroform, respectively). Thus in the production process of micellar nanocrystals, DCM is removed by evaporation much more quickly than chloroform. (2) Tetrahydrofuran (THF), which has much higher miscibility with water compared with chloroform (THF is considered as water-miscible while chloroform as water-immiscible). Thus, in the production process of micellar nanocrystals, the oil-in-water emulsion formed for the chloroform-based process essentially becomes a continuous solution for the THF-based process. Although in each of these two comparative experiments (using chloroform as the reference point), additional solvent properties (other than the primary solvent property varied, namely boiling point and water miscibility, respectively) could also affect the structure of the product to some extent, the respective primary solvent property is believed to be likely the main cause to change the structure of the product considering the fact that the respective primary solvent property has the largest difference compared with that of the reference solvent (chloroform, see ESI Table 1† for the properties of all the organic solvents considered for the present work). It should be noted that the selection space of organic solvents used in the fabrication of micellar nanocrystals is also limited by the following two criteria, *i.e.*, (1) the organic solvent used needs to be able to dissolve both the hydrophobic nanocrystals and the amphiphilic block copolymers with sufficient amounts, and (2) the boiling point of the organic solvent used needs to be lower than that of water. These two selection criteria rule out most of the common organic solvents. ESI Table 1† lists all the organic solvents that we have considered for the present work, from which DCM and THF were selected to be studied further systematically.

In the experiments of comparing DCM *versus* the reference solvent chloroform, the most noticeable difference in the results observed was that, although DCM could still result in successful formation of micelles, nearly all of the formed micelles were empty, *i.e.*, the encapsulation number was virtually zero, based on the transmission electron microscopy (TEM) results (Fig. 1). This indicates that, because DCM is much more volatile than chloroform and DCM leaves the oil-in-water emulsion system much more quickly, with DCM as the organic solvent the micelles don't have sufficient time to encapsulate the hydrophobic nanocrystals before the assembly of empty micelles is complete. This further suggests that, in the assembly process of micellar nanocrystals, the rate of the micelle encapsulation step is quite slow compared with that of the empty micelle assembly step. This is likely to a great extent due to the bulky size of nanocrystals compared with that of polymer molecules (monomers of micelles), rendering the time duration of mass transfer of nanocrystals to gain contact with polymer molecules significant (long enough not to be negligible) compared with that of mass transfer of polymer

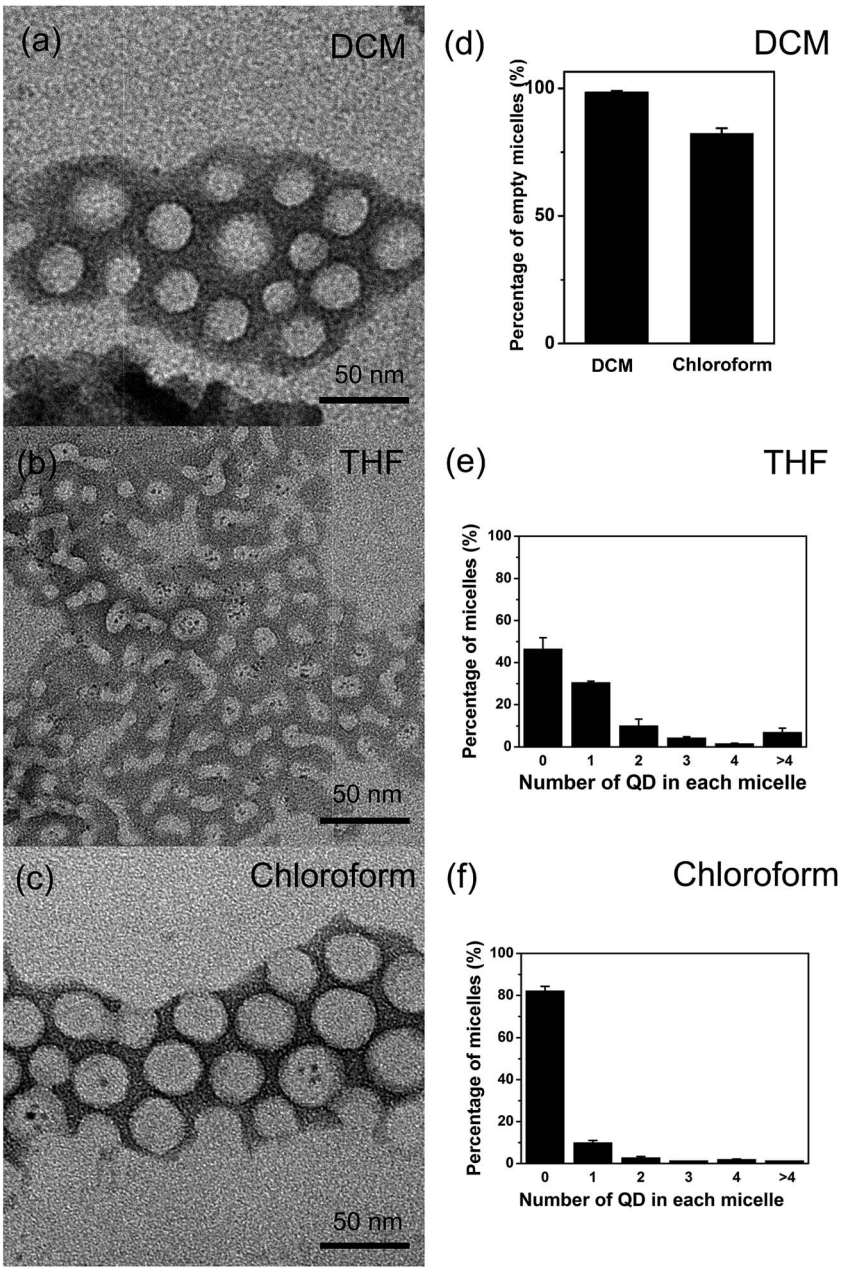

Fig. 1 Effect of DCM and THF *versus* the reference organic solvent chloroform on the encapsulation number of micellar nanocrystals. (a–c) Representative transmission electron microscopy (TEM) images of micelles *via* DCM, THF, and chloroform, respectively. Each of the dark spherical spots (several nanometers in diameter) in the TEM images corresponds to a quantum dot (QD). (d) Percentage of empty micelles when DCM or chloroform was used as the organic solvent. (e and f) Number distribution of nanocrystal-encapsulated micelles with different encapsulation number (number of QD in each micelle) when THF and chloroform, respectively, was used as the organic solvent.

molecules. This reasoning is further supported by the experimental result with another organic solvent diethyl ether, whose boiling point is 34.6 °C and is also much lower than that of chloroform (ESI Fig. 1†). When diethyl ether was used as the organic solvent, it was found that, similar as the encapsulation result given by DCM, virtually all formed micelles were empty (ESI Fig. 1†). It should be noted that, from the point of view of potential of translation to industry, we consider diethyl ether unsafe to be used for industry setting because it is a highly flammable solvent (flash point −45 °C).

In the experiments of comparing THF *versus* the reference solvent chloroform, it was found that THF as the organic solvent greatly enhanced the encapsulation of QDs in micelles, as shown by the dramatic decrease in the percentage of empty micelles (decrease from 82.2 ± 2.9% to 46.5 ± 5.0%, *i.e.*, a nearly twofold reduction, the decrease was determined to be significant at the significance level 5%) and increase in the average number of QDs in each micelle with encapsulated QDs (Fig. 1). This increase in nanocrystal encapsulation by the micelles is important for applications of micellar nanocrystals, and this result shows that adjusting organic solvent could indeed lead to improvement in nanocrystal encapsulation. The most important difference in solvent property between THF and chloroform is the water miscibility: THF is water-miscible while chloroform is water-immiscible (both organic solvents can dissolve QDs and the amphiphilic block copolymer PS–PEG). Thus, THF could greatly facilitate the mass transfer in the assembly 'reaction' system, and enhance encapsulation of QDs into micelles.

Further, it was found that THF as the organic solvent (*versus* chloroform) could also change the physical structure of micelles in the micellar nanocrystal system. For example, THF led to significantly smaller micelle size (Table 1). This result suggests that the micelle size is not only determined by thermodynamics but by kinetics, and once again shows the importance of kinetics *versus* thermodynamics in the assembly process of micellar nanocrystals. Most interestingly, it was found that, when THF was used as the organic solvent, as time went on the nanocrystal-encapsulated micelles changed shape: as the fabrication time increased gradually, more and more worm-shaped nanocrystal-encapsulated micelles and less and less sphere-shaped ones were observed in the product dispersion (Fig. 2a–c). In contrast, this shape-changing phenomenon was not observed for the other organic solvents examined in this work. It should be pointed out that the dispersions of the worm-like micelles were transparent and remained colloidally stable for at least one week.

We further investigated the mechanism of this intriguing shape-changing phenomenon. We hypothesized that the micelle shape change from spherical shape to worm-like shape was due to micelle fusion (Fig. 2d). To check this hypothesis, we performed experiments based on colocalization of hydrophobic dyes with different fluorescent emission colors encapsulated in micelles. In a typical experiment, we first performed the fabrication process of green dye-encapsulated PS–PEG micelles (with

Table 1 Particle size (diameter) characterization for micellar nanocrystals. The 'empty (nm)' and 'loaded (nm)' columns show particle size measurement results by TEM for empty micelles and micelles loaded with QDs, respectively

	TEM (nm)	Empty (nm)	Loaded (nm)	DLS (nm)
DCM	29.0 ± 2.7	29.0 ± 2.7	N/A	N/A
THF	20.8 ± 2.4	20.5 ± 1.1	21.5 ± 1.8	48.8 ± 5.4
Chloroform	34.4 ± 1.2	34.0 ± 1.5	34.6 ± 0.9	74.9 ± 11.3

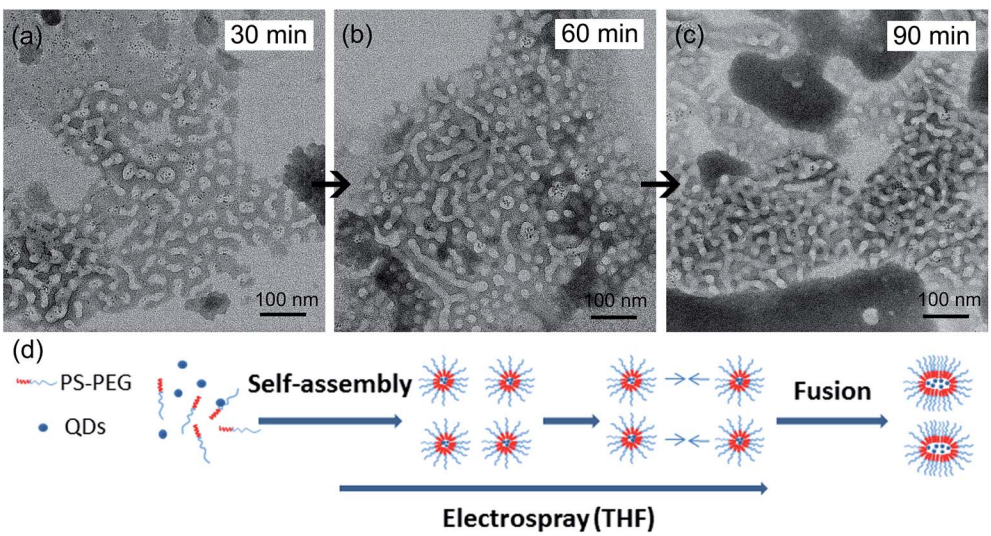

Fig. 2 Nanocrystal-encapsulated micelles changed shape (from spherical to worm-like shape) over time with THF as the organic solvent. (a) TEM image of the nanocrystal-encapsulated micelle product with the electrospray time being 30 min. (b) TEM image of the nanocrystal-encapsulated micelle product with the electrospray time being 60 min. (c) TEM image of the nanocrystal-encapsulated micelle product with the electrospray time being 90 min. The samples of (a), (b), and (c) for TEM were collected from the same production batch, with the only difference between the three samples being the production time. (d) The proposed hypothesis of formation mechanism of worm-shaped micelles.

THF as the organic solvent) based on electrospray combined with self-assembly for 30 min; at 30 min the feeding of green dye (through a syringe pump) was switched to orange dye and the production continued for another 30 min (*i.e.*, totally 60 min). Control experiments were performed to ensure that the fluorescence of the green hydrophobic fluorescent dye only appeared in the green channel of the dual channel (DV2) imaging system (no significant signal detected in the orange-red channel), and the fluorescence of the orange hydrophobic fluorescent dye only appeared in the orange-red channel of the dual channel (DV2) imaging system (no significant signal detected in the orange-red channel, see ESI Fig. 2† for the fluorescent spectra of the two dyes under the excitation wavelength of 488 nm). By confocal fluorescent microscopy we found that the micelle product collected at 30 min showed only green fluorescent color, while at 60 min the micelle product collected showed primarily the composite color of green and orange (Fig. 3). This experimental result is consistent with the micelle fusion hypothesis. It's worth mentioning that control experiments were also performed to show that both dye-encapsulated micelles and empty micelles also exhibit the shape-changing phenomena when THF was used as the organic solvent (ESI Fig. 3†). The reason why QDs were not used for the colocalization study was because the distribution of encapsulation number of QDs in different micelles was far from uniform and many empty micelles formed when QDs were used, which would make the interpretation of experimental results using QDs very difficult; thus small molecule fluorescent dyes were used instead for the colocalization study. Lastly, although we couldn't completely rule out the possibility that part of the hydrophobic dyes was leaked out from the core of one micelle, entered the water phase, and diffused into the core of another micelle, the percentage of this part of the hydrophobic dyes is expected to be very small (much lower than 100%) since hydrophobic dyes favor the hydrophobic environment of the micelle core; and since the colocalization between the green hydrophobic dyes and orange hydrophobic dyes was found to be nearly complete (100%) in the above-mentioned worm-like micelles (Fig. 3, only a small percentage of fluorescent spots in the two separate emission color channels were not colocalized), the predominant cause for the dye colocalization is believed to be fusion of micelles (rather than migration of hydrophobic dyes between the cores of different micelles through the water phase).

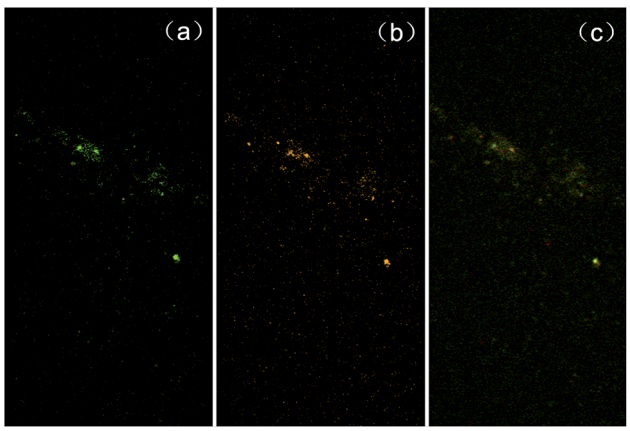

Fig. 3 Colocalization study of the formation mechanism of worm-shaped micelles. A green hydrophobic fluorescent dye and an orange hydrophobic fluorescent dye (with the colors being from the fluorescent emissions) were used in the micelle fabrication process to label the cores of micelles, and by studying the colocalization of the two different fluorescent colors, to examine whether fusion of different micelles labeled with different fluorescent colors had occurred. In the initial 30 min of electrospray, the green hydrophobic fluorescent dye (in addition to PS–PEG) was used in the oil phase flow. Then, after the initial 30 min the dye used was switched to the orange fluorescent dye. (a) Fluorescent image of the micelle product (60 min of electrospray time) through the green color channel of the dual channel (DV2) imaging system; (b) fluorescent image of the micelle product (60 min of electrospray time) through the orange-red color channel of the dual channel (DV2) imaging system; (c) composite image of (a) and (b). Control experiments were performed to ensure that the fluorescence of the green hydrophobic fluorescent dye only appeared in the green channel of the dual channel (DV2) imaging system (no significant signal detected in the orange-red channel), and the fluorescence of the orange hydrophobic fluorescent dye only appeared in the orange-red channel of the dual channel (DV2) imaging system (no significant signal detected in the orange-red channel).

Solvent environment has been previously reported to influence the structure of polymer vesicles, including those containing PS blocks.[26–32] However, using an appropriate organic solvent to induce or facilitate micelle fusion has rarely been reported previously.[33–35] Micelle fusion is an important process of fundamental interest for several fields including biophysics and nanotechnology.[33–35] Thus, the above results suggest a new approach for generating or enhancing micelle fusion. When the organic solvent THF, which is miscible with water and also a good solvent of the glassy hydrophobic block PS of the amphiphilic block copolymer (the Hildebrand solubility parameters of THF and PS are 9.10 $cal^{1/2}$ $cm^{-3/2}$ and 9.13 $cal^{1/2}$ $cm^{-3/2}$, respectively, which are fairly close),[36,37] is used, it could function as a 'bridge' between different micelles, significantly lowering the energy barrier of micelle fusion. Furthermore, worm-shaped micelles are much less common than spherical micelles in nature and it has been reported that worm-shaped micelles could lead to improved tumor targeting effect compared with spherical micelles.[25,38] Using an appropriate organic solvent to help to form worm-shaped micelles has rarely been reported before. Thus, the above results also suggest a new way to produce worm-shaped micelles, including nanocrystal-encapsulated worm-shaped micelles.

In addition to the physical structural properties (size, shape, and encapsulation number) of the micellar nanocrystal product, we also performed experimental studies on its chemical, optical, and biological properties. Thermogravimetric analysis (TGA) of the micellar nanocrystal product gave similar results (ESI Fig. 4†) as those previously reported by Hayward *et al.*,[25] indicating similar chemical compositions. Fluorescent spectroscopy results showed that the micellar nanocrystal product largely maintained the fluorescent property of the hydrophobic QDs used in the reactants (ESI Fig. 5†).

Worm-like micelles, which are sometimes also called 'filomicelles', have been previously reported to offer several important

advantages compared with the spherical counterparts in biomedical applications, such as reduced non-specific cellular uptake, prolonged blood circulation time, and enhanced drug delivery.[39–41] Here, we performed preliminary experiments to examine the potential advantages of the worm-like micelles formed by THF-induced/facilitated micelle fusion in reducing non-specific cellular uptake. First, we conjugated the micellar nanocrystal product with Tat peptide (part of PS–PEG was replaced by PS–PEG–COOH in the micellar nanocrystal formation process), which is known to have high cellular delivery efficiency for a variety of microscopic cargos,[42–45] and found that the thus-obtained biofunctionalized micellar nanocrystals could be internalized by live HeLa cells with high efficiency (Fig. 4), thus demonstrating feasibility of these micellar nanocrystals for applications in biological systems. Further, we found that the worm-shaped QD-encapsulated micelles formed *via* THF led to dramatically reduced cellular uptake, compared with the spherical QD-encapsulated micelles formed *via* chloroform (Fig. 4). Conjugating the worm-shaped micellar QDs with Tat peptide was found to significantly enhance the cellular uptake (Fig. 4). These results thus suggest the potential of the worm-like micelles formed *via* THF in minimizing non-specific cellular uptake and enhancing the targeting effects in applying the nanomaterials for biomedical imaging, drug delivery, and detection.

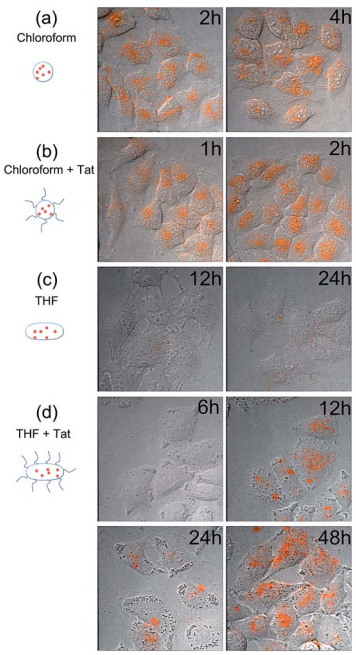

Fig. 4 Imaging of cellular uptake and transport of micellar QDs. Each image is a composite of a bright field image and the corresponding fluorescent confocal image (the orange color is from the fluorescence of QDs) of HeLa cells after incubation with micellar QDs of different structures for different time durations (fresh culture medium was used to wash away the extracellular micellar QDs at the different time points of incubation). (a) Micellar QDs prepared with chloroform as the organic solvent, which thus had spherical shape; (b) Tat peptide-conjugated micellar QDs prepared with chloroform as the organic solvent, which thus had spherical shape; (c) micellar QDs prepared with THF as the organic solvent and with 90 min of electrospray time, which thus had worm shape; (d) Tat peptide conjugated micellar QDs prepared with THF as the organic solvent and with 90 min of electrospray time, which thus had worm shape.

Conclusions

In the present work, we used electrospray combined with self-assembly to fabricate micellar nanocrystals, with QDs as the model nanocrystals. We investigated the effects of organic solvents on the properties (especially the physical structural properties) of the product. It was found that DCM, which evaporates much faster than the reference organic solvent chloroform, led to empty micelles, and that THF, which has much greater water miscibility than chloroform, greatly enhanced nanocrystal encapsulation into micelles. Furthermore, we discovered an interesting shape-changing phenomenon for the micelles produced with THF being used as the organic solvent. Two-color dye colocalization studies suggest that the likely mechanism for this phenomenon is solvent-induced/facilitated micelle fusion, which could offer a new approach to induce/facilitate fusion of self-assembled structures and a new way to produce worm-shaped micelles. The thus-produced worm-shaped micelles were found to offer greatly reduced non-specific cellular uptake compared with the spherical micelle counterparts. The results obtained here provide significant insights on the emerging class of nanomaterials named micellar nanocrystals, including highlighting the importance of kinetics *versus* thermodynamics in the fabrication process, and provide potential means to control the structure of micellar nanocrystals as well as their biological behaviors for biomedical applications.

Acknowledgements

The authors gratefully acknowledge the financial support of a “Thousand Young Global Talents” award from the Chinese Central Government, a “Shuang Chuang” award from the Jiangsu Provincial Government, start-up fund from College of Engineering and Applied Sciences, Nanjing University, China, award from the “Tian-Di” Foundation, grant from the Priority Academic Program Development Fund of Jiangsu Higher Education Institutions (PAPD).

References

1 S. Nie, Y. Xing, G. J. Kim and J. W. Simons, *Annu. Rev. Biomed. Eng.*, 2007, **9**, 257–288.
2 A. M. Smith, G. Ruan, M. N. Rhyner and S. Nie, *Ann. Biomed. Eng.*, 2006, **34**, 3–14.
3 J. R. Heath and M. E. Davis, *Annu. Rev. Med.*, 2008, **59**, 251–265.
4 K. Pu, N. Chattopadhyay and J. Rao, *J. Controlled Release*, 2016, **240**, 312–322.
5 M. Swierczewska, H. S. Han, K. Kim, J. H. Park and S. Lee, *Adv. Drug Delivery Rev.*, 2016, **99**, 70–84.
6 X. Gao, L. Yang, J. A. Petros, F. F. Marshall, J. W. Simons and S. Nie, *Curr. Opin. Biotechnol.*, 2005, **16**, 63–72.
7 A. N. Lukyanov and V. P. Torchilin, *Adv. Drug Delivery Rev.*, 2004, **56**, 1273–1289.

8 B. Dubertret, P. Skourides, D. J. Norris, V. Noireaux, A. H. Brivanlou and A. Libchaber, *Science*, 2002, **298**, 1759–1762.
9 G. Ruan, G. Vieira, T. Henighan, A. Chen, D. Thakur, R. Sooryakumar and J. O. Winter, *Nano Lett.*, 2010, **10**, 2220–2224.
10 G. Ruan and J. O. Winter, *Nano Lett.*, 2011, **11**, 941–945.
11 J.-H. Park, G. von Maltzahn, E. Ruoslahti, S. N. Bhatia and M. J. Sailor, *Angew. Chem.*, 2008, **120**, 7394–7398.
12 M. J. Sailor and J.-H. Park, *Adv. Mater.*, 2012, **24**, 3779–3802.
13 L. Jing, K. Ding, S. V. Kershaw, I. M. Kempson, A. L. Rogach and M. Gao, *Adv. Mater.*, 2014, **26**, 6367–6386.
14 G. Bao, S. Mitragotri and S. Tong, *Annu. Rev. Biomed. Eng.*, 2013, **15**, 253–282.
15 S. Mura and P. Couvreur, *Adv. Drug Delivery Rev.*, 2012, **64**, 1394–1416.
16 A. Louie, *Chem. Rev.*, 2010, **110**, 3146–3195.
17 R. Nagarajan, *Polym. Adv. Technol.*, 2001, **12**, 23–43.
18 R. Nagarajan and K. Ganesh, *J. Chem. Phys.*, 1993, **98**, 7440–7450.
19 P. Lim Soo, L. Luo, D. Maysinger and A. Eisenberg, *Langmuir*, 2002, **18**, 9996–10004.
20 Y. Zhao, F. Fay, S. Hak, J. Manuel Perez-Aguilar, B. L. Sanchez-Gaytan, B. Goode, R. Duivenvoorden, C. de Lange Davies, A. Bjørkøy, H. Weinstein, Z. A. Fayad, C. Pérez-Medina and W. J. M. Mulder, *Nat. Commun.*, 2016, **7**, 11221.
21 V. Patel, J. Dey, R. Ganguly, S. Kumar, S. Nath, V. K. Aswal and P. Bahadur, *Soft Matter*, 2013, **9**, 7583–7591.
22 Y. Mai and A. Eisenberg, *Chem. Soc. Rev.*, 2012, **41**, 5969–5985.
23 A. D. Duong, G. Ruan, K. Mahajan, J. O. Winter and B. E. Wyslouzil, *Langmuir*, 2014, **30**, 3939–3948.
24 J. Zhu and R. C. Hayward, *J. Am. Chem. Soc.*, 2008, **130**, 7496–7502.
25 J. Bae, J. Lawrence, C. Miesch, A. Ribbe, W. Li, T. Emrick, J. Zhu and R. C. Hayward, *Adv. Mater.*, 2012, **24**, 2735–2741.
26 D. E. Discher and A. Eisenberg, *Science*, 2002, **297**, 967.
27 H. Shen and A. Eisenberg, *J. Phys. Chem. B*, 1999, **103**, 9473–9487.
28 I. A. Maxwell and J. Kurja, *Langmuir*, 1995, **11**, 1987–1993.
29 L. Luo and A. Eisenberg, *J. Am. Chem. Soc.*, 2001, **123**, 1012–1013.
30 L. Luo and A. Eisenberg, *Langmuir*, 2001, **17**, 6804–6811.
31 D. A. Wilson, R. J. M. Nolte and J. C. M. van Hest, *Nat. Chem.*, 2012, **4**, 268–274.
32 J. Li, I. Rozen and J. Wang, *ACS Nano*, 2016, **10**, 5619–5634.
33 Y. Rharbi, M. Li, M. A. Winnik and K. G. Hahn, *J. Am. Chem. Soc.*, 2000, **122**, 6242–6251.
34 M. H. Repollet-Pedrosa and M. K. Mahanthappa, *Soft Matter*, 2013, **9**, 7684–7687.
35 T. H. Kim, J. Huh, J. Hwang, H.-C. Kim, S. H. Kim, B.-H. Sohn and C. Park, *Macromolecules*, 2009, **42**, 6688–6697.
36 https://en.wikipedia.org/wiki/Hildebrand_solubility_parameter.
37 M. Belmares, M. Blanco, W. A. Goddard, R. B. Ross, G. Caldwell, S. H. Chou, J. Pham, P. M. Olofson and C. Thomas, *J. Comput. Chem.*, 2004, **25**, 1814–1826.
38 J.-H. Park, G. von Maltzahn, L. Zhang, M. P. Schwartz, E. Ruoslahti, S. N. Bhatia and M. J. Sailor, *Adv. Mater.*, 2008, **20**, 1630–1635.
39 N. S. Oltra, P. Nair and D. E. Discher, *Annu. Rev. Chem. Biomol. Eng.*, 2014, **5**, 281–299.
40 S. M. Loverde, M. L. Klein and D. E. Discher, *Adv. Mater.*, 2012, **24**, 3823–3830.
41 Y. Geng, P. Dalhaimer, S. Cai, R. Tsai, M. Tewari, T. Minko and D. E. Discher, *Nat. Nanotechnol.*, 2007, **2**, 249–255.
42 G. Ruan, A. Agrawal, A. I. Marcus and S. Nie, *J. Am. Chem. Soc.*, 2007, **129**, 14759–14766.
43 H. Brooks, B. Lebleu and E. Vivès, *Adv. Drug Delivery Rev.*, 2005, **57**, 559–577.
44 B. Gupta, T. S. Levchenko and V. P. Torchilin, *Adv. Drug Delivery Rev.*, 2005, **57**, 637–651.
45 A. Joliot and A. Prochiantz, *Nat. Cell Biol.*, 2004, **6**, 189–196.

